



# Aqueous Synthesis and Stability of Two-dimensional Halide Perovskites

**Jisung Seo, Alexander Jess, Ruiquan Yang, & Charles Hages**

*Department of Chemical Engineering*

Faculty Mentor: Charles Hages, Department of Chemical Engineering

## Abstract

2D perovskite's quantum confinement and superlattices enhance electron and hole recombination which maximizes the photoluminescence quantum efficiency for optical devices. The water stability of perovskites, however, is remained unresolved. Perovskite water stability requires ligands that are nonpolar and have strong intermolecular forces as nonpolar surface push water away from the perovskite and their strong intermolecular force prevent water from permeating in between the ligands. Amino functionalized aliphatic chain ligand serves as a robust candidate as long carbon chains are nonpolar, cohesive, and has low electron affinity. Furthermore, the nonpolar active sites create paths to interact with other nonpolar chemicals such as nitrogen bases of DNAs. Here, we demonstrate tin and lead based organic-inorganic halide 2D perovskite's – capped with eight carbon long aliphatic chains – optical and structural properties. Self-assembly of tin-based perovskites showed near-unity photoluminescence quantum yield but had poor stability in water or ambient condition due to hydrolysis whereas lead-based perovskites showed less PL but were stable in water at high concentrations. With better stability, lead  $\text{OA}_2\text{PbI}_4$  perovskite's optical characteristics before and after conjugating with Adenosine were further studied. Hydrophobic interaction between the perovskite and the Adenosine was insufficient to alter the bandgap, and no major light energy or intensity change has been detected to operate as a biological sensor.

*Keywords:* quantum confinement, photoluminescence (PL), perovskite, 2D, optical characteristic

## Introduction

2D perovskites have a structure of  $\text{A}_2\text{BX}_4$  layers where A are cations that have long aliphatic chains, B are metals, and X are halides. They are known for their superb optical characteristic with electron quantum confinement from quantum well structure followed by superlattices (Gao et al., 2019)(Blancon et al., 2018). Quantum confinement allows charge carriers to interact stronger due to Coulomb forces that enhance electrons and holes recombination (Ishihara et al., 1989)(Papavassiliou, 1997). This phenomenon maximizes the photoluminescence quantum efficiency (PLQY) and has stimulated the use of perovskites in optoelectronic applications including photodetectors, light-emitting diodes (LED), and lasers (Wang et al., 2019)(Tan et al., 2016)(Qin et al., 2020). As opposed to their optical advantages, however, water stability of perovskites is remained unresolved.

The chronic drawback of the halide perovskites is hydrolysis in water or ambient condition with the presence of oxidizing source (Jana et al., 2019)(Yang et al., 2019). Numerous experimental approaches have been conducted to prevent hydrolysis such as growing hydroxide passivating outer layer (Jana & Kim, 2018) and encapsulating with polymers (Lee et al., 2018)(Kim et al., 2019). But preventive layer around the perovskite does not resolve intrinsic vulnerability of the perovskites. Gao et al. successfully designed water-stable hydrophobic organic ligand capped perovskites without an additional outer layer (Gao et al., 2019). BTM, a sophisticatedly engineered organic capping ligand, self-interacts strongly with intermolecular  $\pi$ - $\pi$  interactions that minimize water permeation accompanied by cation dissolution. However, the electrons from inorganic layer are quenched to organic BTM, thus red PL is emitted from the BTM-lead iodide perovskite regardless of the formation of the perovskite whereas intrinsic green PL should be detected for lead iodide perovskites.

Perovskite water stability requires two critical factors: nonpolar ligand and strong intermolecular forces. Nonpolar ligand push water away from the perovskite and their strong intermolecular force prevents water from permeating in between the ligands (Gao et al., 2019). In this regard, the amino functionalized aliphatic chain serves as a robust candidate as long carbon chains are nonpolar and cohesive (Koh et al., 2018). Besides, as opposed to the BTM ligand, aliphatic chains have low electron affinity that preserves emission from the inorganic layer. Furthermore, the nonpolar outer surface region function as active sites for other nonpolar chemicals. Husale et al. indicated that the DNA's inner structure nitrogen bases are nonpolar (Husale et al., 2008), and the conjugation of nucleosides or other biochemicals to the optically active perovskite is potential for aqueous biological devices.

In this work, we demonstrate multifaceted approaches for the synthesis of tin and lead-based perovskites with octylamine ligand and diverse halide sources. The tin-based perovskites have excellent photoluminescence quantum yield but unstable in water or ambient condition due to hydrolysis whereas lead-based perovskites have less PLQY but are stable in water at high concentrations. In essence, we demonstrate the conjugation process between the perovskite and the nucleoside, and resultant optical discrepancy to further study whether it can operate as biological devices.

## Materials and Methods

### Materials

SnBr<sub>2</sub> (100%), SnCl<sub>2</sub> (98%), n-octylamine (OA) ( $\geq 99\%$ ), H<sub>3</sub>PO<sub>2</sub> (50% wt. in H<sub>2</sub>O), Hydrobromic acid (HBr) (48% wt. in H<sub>2</sub>O), Hydroiodic acid (HI) ( $\geq 47\%$  wt. in H<sub>2</sub>O and  $\leq 1.5\%$  H<sub>3</sub>PO<sub>2</sub>) were purchased from Sigma-Aldrich. SnO (99.9%), PbBr<sub>2</sub> ( $\geq 98\%$ ), PbCl<sub>2</sub> (99%), PbI<sub>2</sub> (99.9985%), Hydrochloric acid (HCl) ( $\geq 37\%$ ) were purchased from Fisher-Scientific.

### Materials Synthesis

#### Synthesis of 2D OA<sub>2</sub>SnBr<sub>4</sub>

The solution was carried out in the ambient condition. SnO (101.0 mg, 0.75 mmol) was dissolved with HBr (2.5 mL) and H<sub>3</sub>PO<sub>2</sub> (15 mL) in round bottom flask (RBF), and the solution was sonicated for 5 minutes to fully dissolve SnO particles. After the precursors were fully dissolved, OA (0.475 mL) was injected under strong agitation with stirring and the solution was heated to 80°C for 30 minutes. It was cooled to room temperature slowly in ambient air and was put in an ice bath to further crystallize. If the ice is not prepared, liquid nitrogen is an alternative cooling method. When the solution is slowly cooled in ice bath, white crystals were formed, but when the solution was quickly cooled with liquid nitrogen, yellow crystals with partial oxidation were formed. Defects for yellow crystals were reduced and they were dried in vacuum. The perovskites had a strong yellow PL.

#### Synthesis of 2D OA<sub>2</sub>SnI<sub>4</sub>

The solution was carried out in the ambient condition. SnO (101.0 mg, 0.75 mmol) was dissolved with HBr (2.5 mL) and H<sub>3</sub>PO<sub>2</sub> (15 mL) in RBF, and the solution was sonicated for 5 minutes to fully dissolve SnO particles. After the precursors were fully dissolved, OA (0.475 mL) was injected under strong agitation with stirring and the solution was heated to 80°C for 30 minutes. It was cooled to room temperature slowly in ambient air and was put in an ice bath to further crystallize. When OA<sub>2</sub>SnBr<sub>4</sub> perovskites were formed, HI was injected slowly under strong stirring until the halide exchange occurred. The OA<sub>2</sub>SnI<sub>4</sub> perovskites turned dark red and had strong red-orange PL.

#### Synthesis of 2D OA<sub>2</sub>PbCl<sub>4</sub>

The solution was carried out in the glove box. PbCl<sub>2</sub> (69.53 mg, 0.25 mmol) was dissolved with HCl (5 mL) in RBF, and the solution was sonicated for 5 minutes to fully dissolve PbCl<sub>2</sub> particles. After the precursors were fully dissolved, OA (0.165 mL) was injected under strong

agitation with stirring and the solution was heated to 80°C for 30 minutes. It was cooled to room temperature slowly in ambient air and was put in an ice bath to further crystallize.

### Synthesis of 2D OA<sub>2</sub>PbBr<sub>4</sub>

The solution was carried out in the glove box. PbBr<sub>2</sub> (91.75 mg, 0.25 mmol) was dissolved with HBr (5 mL) in RBF, and the solution was sonicated for 5 minutes to fully dissolve PbBr<sub>2</sub> particles. After the precursors were fully dissolved, OA (0.165 mL) was injected under strong agitation with stirring and the solution was heated to 80°C for 30 minutes. It was cooled to room temperature slowly in ambient air and was put in an ice bath to further crystallize.

### Synthesis of 2D OA<sub>2</sub>PbI<sub>4</sub>

The solution was carried out in the glove box. PbI<sub>2</sub> (115.25 mg, 0.25 mmol) was dissolved with HI (5 mL) in RBF, and the solution was sonicated for 5 minutes to fully dissolve PbI<sub>2</sub> particles. After the precursors were fully dissolved, OA (0.165 mL) was injected under strong agitation with stirring and the solution was heated to 80°C for 30 minutes. It was cooled to room temperature slowly in ambient air and was put in an ice bath to further crystallize.

## Results and Discussion

### OA<sub>2</sub>SnX<sub>4</sub> Perovskites

For OA<sub>2</sub>SnBr<sub>4</sub> synthesis, the role of H<sub>3</sub>PO<sub>2</sub> was experimented with various concentrations during the synthesis. For the reaction, as soon as SnBr<sub>2</sub> precursor was added into HBr, the solution became murky yellow, but as H<sub>3</sub>PO<sub>2</sub> was added, the solution became clear, implying that the hydrolysis of the tin precursor is reduced.

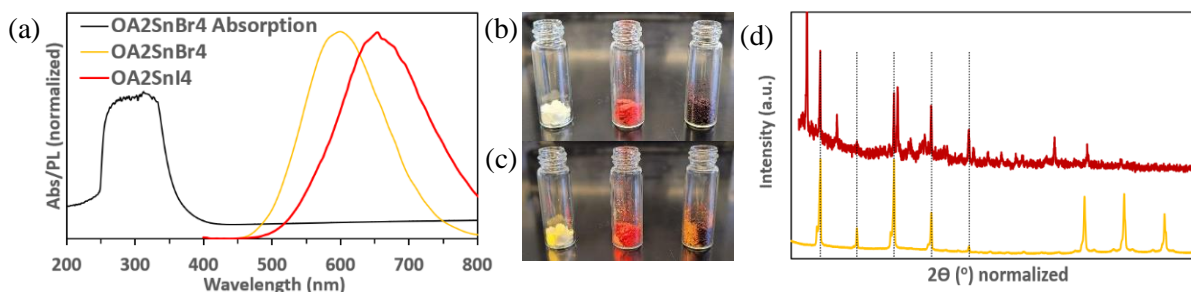


**Figure 1.** (a) Absorption and emission for OA<sub>2</sub>SnBr<sub>4</sub> and OA<sub>2</sub>SnI<sub>4</sub> perovskites. (b) Photographs of OA<sub>2</sub>SnBr<sub>4</sub>, OA<sub>2</sub>SnBrI, and OA<sub>2</sub>SnI<sub>4</sub> perovskites from left to right respectively without UV light. (c) OA<sub>2</sub>SnBr<sub>4</sub>, OA<sub>2</sub>SnBrI, and OA<sub>2</sub>SnI<sub>4</sub> perovskites from left to right respectively with UV light. (d) X-Ray Diffraction (XRD) pattern for OA<sub>2</sub>SnI<sub>4</sub> (red) and OA<sub>2</sub>SnBr<sub>4</sub> (yellow)

The optical characteristics of OA<sub>2</sub>SnBr<sub>4</sub> and OA<sub>2</sub>SnI<sub>4</sub> perovskites were measured through UV-Vis absorption and PL spectroscopy as shown in Figure 1 (a). For OA<sub>2</sub>SnBr<sub>4</sub>, major

absorption widely ranged between 250 nm to 350 nm, and the PL spectrum was centered at 600 nm indicating that the bandgap of the perovskite is around 2.07 eV. For  $\text{OA}_2\text{SnI}_4$ , the PL spectrum was centered at 660 nm indicating that the bandgap of the perovskite is 1.88 eV. These emissions are well depicted with the photographs of  $\text{OA}_2\text{SnX}_4$  perovskites illustrated in Figure 1 (b). In order to observe the tunability of the  $\text{OA}_2\text{SnX}_4$  perovskite,  $\text{OA}_2\text{SnBr/I}$  and  $\text{OA}_2\text{SnI}_4$  perovskites were synthesized through halide exchange. As the amount of iodide source dictated the perovskite's octahedra, PL shifted from yellow to dark orange. The wavelength trend for PL is consistent with previous reports that the higher the order of the halide source, the longer the wavelength of perovskite's PL. Structure dependency for wavelength variation trend is not dominant because they are also well-spotted for 3D perovskites, rather, the electron affinity of halides that resist electrons to recombine to produce PL is the key shifting emission peaks.

The 2D crystal structure of  $\text{OA}_2\text{SnX}_4$  perovskites was verified by XRD as shown in Figure 1 (d). The miller indices of 2D perovskite plane were calculated via de Broglie equation as shown in Table 1. As the interval of  $2\theta$  for  $\text{OA}_2\text{SnBr}_4$  is about  $4.5^\circ$ , (001) and (002) planes are expected to be in the lower  $\theta$  value. Similarly,  $5.5^\circ$  spacing was observed and (001) peak would ideally be at  $5.5^\circ$ . From the interlayer spacing calculation, iodide placed perovskite showed smaller interlayer spacing based on Bragg's law. This could be resulted from the larger size of the iodide octahedron compared to bromine that creates more space for OA to intermesh closely.

**Table 1.** Miller indices calculation for (a)  $\text{OA}_2\text{SnBr}_4$  and (b)  $\text{OA}_2\text{SnI}_4$  with de Broglie equation

$2\theta$	$\sin^2(\theta)$	$S_n/S_1$ Ratio	Plane
(a) $\text{OA}_2\text{SnBr}_4$			
4.5	0.0015	1	(001)
9.0	0.006	4.0	(002)
13.56	0.014	9.3	(003)
18.02	0.0245	16.2	(004)
22.44	0.0379	25.2	(005)
26.98	0.0544	36.2	(006)
(b) $\text{OA}_2\text{SnI}_4$			
5.5	0.0023	1	(001)
11.2	0.0095	4.1	(002)
16.73	0.0212	9.2	(003)
22.26	0.0373	16.2	(004)
27.84	0.0579	25.2	(005)

Moreover, the stability of  $\text{OA}_2\text{SnBr}_4$  was experimented with various solvents: water, hexane,  $\text{HBr}$ , DMF, and OA. With few drops of water, white  $\text{OA}_2\text{SnBr}_4$  particles turned yellow and instantaneously lost their PL regardless of the concentration. In hexane, the perovskite's PL was reduced and turned orange. After hexane was removed, the perovskite went back to its original condition. In  $\text{HBr}$ , the perovskite did not disperse well, so sonication was used to disperse them. When sonicated, the crystals turned white and had no PL. In DMF and OA, the perovskite instantaneously dissolved, and the PL was gone and the particles were fully dissolved. Tin metal spontaneously oxidizes from oxidation source, and this intrinsic instability is well depicted for tin-based perovskites in various solvents except hexane.

### $\text{OA}_2\text{PbX}_4$ Perovskites

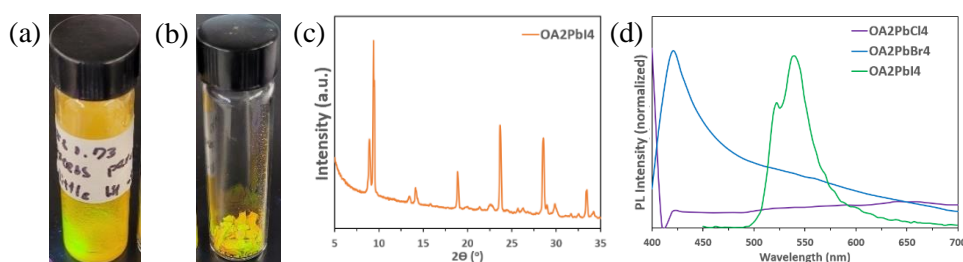


**Figure 2.** (a) Photograph of  $\text{OA}_2\text{PbI}_4$  in water after 1 year (b) Photograph of  $\text{OA}_2\text{PbI}_4$  in ambient air after 1 year. (c) XRD of  $\text{OA}_2\text{PbI}_4$ . (d) PL emission of  $\text{OA}_2\text{PbCl}_4$ ,  $\text{OA}_2\text{PbBr}_4$ , and  $\text{OA}_2\text{PbI}_4$  from left to right respectively.

$\text{OA}_2\text{PbX}_4$  synthesis was carried out in the glove box as lead halide precursors are air sensitive. However, once the perovskite synthesis is done, their stability in ambient air and water is dramatically improved than tin-based OA capped perovskites. Figure 2 (a) and (b) illustrate the PL for  $\text{OA}_2\text{PbI}_4$  perovskite in water and ambient air for more than 1 year with photographs. However, for the instantaneous hydrolysis, the amount of  $\text{OA}_2\text{PbI}_4$  perovskite turned into  $\text{PbI}_2$  with a proportional amount of water.  $\text{OA}_2\text{PbI}_4$ 's time-resolved water stability and detail characterization will be further explained under 3.7.

The crystal structure of  $\text{OA}_2\text{PbI}_4$  was verified by PXRD measurement presented in Figure 2 (b). The repetitive major XRD peaks intervals of  $4.7^\circ$  for  $9.36^\circ$ ,  $14.08^\circ$ ,  $18.9^\circ$ ,  $23.68^\circ$ ,  $28.48^\circ$ , and  $33.5^\circ$  peaks demonstrate that the perovskite has (00X) plane similar to  $\text{OA}_2\text{SnBr}_4$  which is in z-direction confirming that the perovskite is 2D, separated by aliphatic chain capping ligands. Commonly, when the electronegativity of halides is decreased, the PL is shifted to the right, meaning that the wavelength gets longer, and the trend is well demonstrated in Figure 2(a). Both  $\text{OA}_2\text{PbCl}_4$  and  $\text{OA}_2\text{PbBr}_4$  had white color without UV, and under UV,  $\text{OA}_2\text{PbCl}_4$  had PL exciton

peak at 400 nm at the lowest as expected and  $\text{OA}_2\text{PbBr}_4$  had PL at 420 nm. Interestingly, as shown in Figure 2 (a) and (c)  $\text{OA}_2\text{PbI}_4$  had orange color without UV and had green PL under UV which is analogous to 3D  $\text{MAPbBr}_3$  perovskite although the halide electronegativity increased. Such phenomenon can be explained by quantum confinement that encourages exciton oscillation strength for the 2D structure to the out-of-plane direction that results in increasing the bandgap (Gao et al., 2019),(Deng et al., 2020),(Xing et al., 2017).

### $(\text{OA})_2\text{PbI}_4$ Nucleoside conjugation

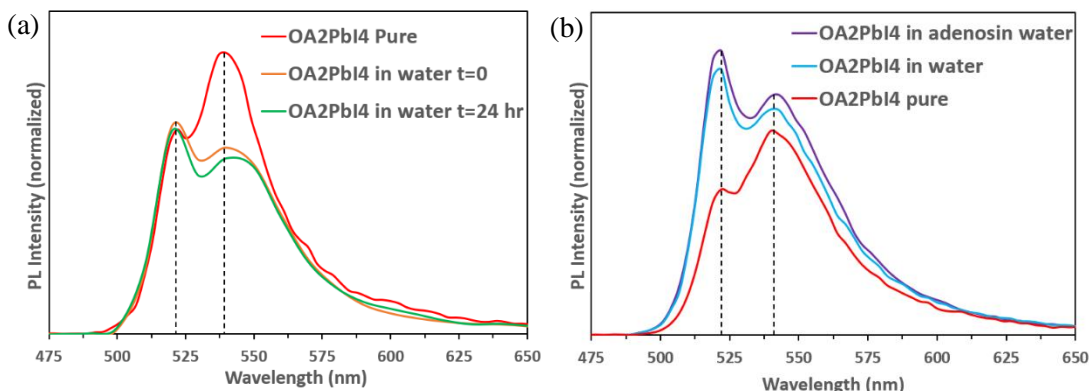


**Figure 3.** (a) PL intensity of  $\text{OA}_2\text{PbI}_4$  perovskites without water addition, in water at  $t=0$  hour, in water at  $t=24$  hours from top to bottom, respectively. (b) PL intensity of  $\text{OA}_2\text{PbI}_4$  perovskites in adenosine dispersed water at  $t=0$  hour, in pure water at  $t=0$  hour, and without water addition from top to bottom, respectively.

The stability of  $\text{OA}_2\text{PbI}_4$  perovskite was studied by comparing PL intensities in various conditions that were measured at equivalent conditions such as exposure time, binning, and wavelength intervals. Figure 3 (a) demonstrates  $\text{OA}_2\text{PbI}_4$  perovskite that was not in contact with water, in water at time = 0, and in water at time = 24hr. Noticeably, the emission feature illustrates that  $\text{OA}_2\text{PbI}_4$  has two peaks at 540 nm and 520 nm that are not detected from other 3D perovskites. 2D perovskite's planar structure generates distinct electromagnetic momentum (EM) in different polarized directions, and photoluminescence spectra of polarized in perpendicular and parallel directions were well studied by DeCrescent (DeCrescent et al., 2020). Both emission peaks at 520 nm and 540 nm correspond to the polarized spectra in the perpendicular direction to the 2D plane while the peak at 520 nm only corresponds to the parallel direction. This is supported by the energy state of the emission in the perpendicular direction that photons are less hindered to escape while 2D planar geometry inhibits and traps lights in oblique angles. Such highly anisotropic-dependent electron polarization and directionality is a concern for 2D materials as the light energy cannot be finely tuned.

Compared to the trend in a dried condition, the emission at 520 nm is superior to 540 nm when  $\text{OA}_2\text{PbI}_4$  was dispersed in water. This illustrates that the water diminishes light trapping and amplifies the PL yield in a parallel direction to the planar. The overall PLQY intensity was decreased in Figure 3 (a) when  $\text{OA}_2\text{PbI}_4$  perovskite was dispersed in water, but as only a few amounts of the perovskite were presented, with the proportional amount of water, PL was decreased from the decomposition of the perovskite. Figure 3 (b) illustrates the opposite trend that the overall PL intensity was increased in addition to water. Such a trend is more reasonable as the water addition increased the emission intensity at 520 nm. Additionally, DeCrescent examined the PL based on polarization and directionality with a shorter aliphatic chain capping ligand. In his research, 4-carbon chain amino-functionalized ligand was used, but the emission features are identical to the 8-carbon chain ligand. Therefore, in 2D materials, crystal structure dominates optical characteristics not the length of the ligand.

Moreover, in order to characterize the interaction between nonpolar aliphatic chain capping ligand and the nucleoside, highly concentrated adenosine dispersed water was added to  $\text{OA}_2\text{PbI}_4$  perovskite. Although adenosine has its excitation close to 400 nm by absorbing UV source, no significant intensity or PL shifting has occurred. Definite PL discrepancy is required when conjugated with nucleosides to detect DNA breakage, but no notable change has been detected. For better results, a nanoscale designed experiment may improve demonstrating the nucleoside-aliphatic chain interaction, but it is conflicting with the stability of perovskites in a low concentration condition and the reason for pioneering facile and convenient detection technique.

### **Conclusion**

In summary, we have demonstrated plain aliphatic chain organic-inorganic tin and lead based perovskites. Their 2D crystallinity was confirmed with x-ray diffraction measurement, PLQY was measured with optical detector, and water stability was experimented by immersing perovskites in ultra-pure water. Notably,  $\text{OA}_2\text{PbI}_4$  perovskite's PL came from inorganic layer and showed great water stability in water. However, 2D multiple emission feature is challenging to finely tune the PL, water stability is diminished when substantially diluted with water, and no significant PL intensity change or emission feature shifting was observed, therefore conflicting with the purpose of engineering facile, convenient, and stable optical device. We foresee this work will encourage to further interdisciplinary studies on 2D perovskites for biological applications and develop all-around capable optical devices.

### Acknowledgements

I would like to express my special thanks of gratitude to my advisor, Dr. Charles Hages for giving me a great opportunity and the guidance to successfully complete this project over past years. Through his meticulous care and support, I have accumulated essential research skills and learned the art of interdisciplinary studies. From our research group, I would like to extend my gratitude to Ph.D. candidates Alexander Jess and Ruiquan Yang for numerous sample characterizations and their research guidance. This research was funded by University Scholars Program by the University of Florida.

### References

- Blancon, J.-C., Stier, A. V., Tsai, H., Nie, W., Stoumpos, C. C., Traore, B., Pedesseau, L., Kepenekian, M., Katsutani, F., Noe, G. T., Kono, J., Tretiak, S., Crooker, S. A., Katan, C., Kanatzidis, M. G., Crochet, J. J., Even, J., & Mohite, A. D. (2018). Scaling law for excitons in 2D perovskite quantum wells. *Nature Communications*, *9*(2254). <https://doi.org/https://doi.org/10.1038/s41467-018-04659-x>
- DeCrescent, R., Venkatesan, N., Dahlman, C., Kennard, R., Zhang, X., Li, W., Du, X., Chabinyk, M., Zia, R., & Schuller, J. (2020). Bright magnetic dipole radiation from two-dimensional lead-halide perovskites. *Science Advances*, *6*(6). <https://doi.org/10.1126/sciadv.aay4900>
- Deng, S., Shi, E., Yuan, L., Jin, L., Dou, L., & Huang, L. (2020). Long-range exciton transport and slow annihilation in two-dimensional hybrid perovskites. *Nature Communications*, *11*(1), 664. <https://doi.org/10.1038/s41467-020-14403-z>
- Gao, Y., Shi, E., Deng, S., Shiring, S., Snaider, J., Liang, C., Yuan, B., Song, R., & Janke, S. (2019). Molecular engineering of organic–inorganic hybrid perovskites quantum wells. *Nature Chemistry*, *11*, 1151–1157. <https://doi.org/https://doi.org/10.1038/s41557-019-0354-2>
- Husale, S., Grange, W., Karle, M., Burgi, S., & Hegner, M. (2008). Interaction of cationic surfactants with DNA: a single-molecule study. *Nucleic Acids Research*, *36*(5), 1443–1449. <https://doi.org/10.1093/nar/gkm1146>
- Ishihara, T., Takahashi, J., & Goto, T. (1989). Exciton state in two-dimensional perovskite semiconductor (C<sub>10</sub>H<sub>21</sub>NH<sub>3</sub>)<sub>2</sub>PbI<sub>4</sub>. *Solid State Communications*, *69*(9), 933–936. [https://doi.org/10.1016/0038-1098\(89\)90935-6](https://doi.org/10.1016/0038-1098(89)90935-6)
- Jana, A., Ba, Q., & Kim, K. S. (2019). Compositional and Dimensional Control of 2D and Quasi-2D Lead Halide Perovskites in Water. *Advanced Functional Materials*, *29*(28). <https://doi.org/10.1002/adfm.201900966>
- Jana, A., & Kim, K. S. (2018). Water-Stable, Fluorescent Organic–Inorganic Hybrid and Fully Inorganic Perovskites. *ACS Energy Letters*, *3*(9), 2120–2126.

<https://doi.org/10.1021/acseenergylett.8b01394>

- Kim, H., Lee, J., Kim, B., Byun, H. R., Kim, S. H., Oh, H. M., Baik, S., & Jeong, M. seok. (2019). Enhanced Stability of MAPbI<sub>3</sub> Perovskite Solar Cells using Poly(p-chloroxylylene) Encapsulation. *Scientific Reports*, 9(15461). <https://doi.org/10.1038/s41598-019-51945-9>
- Koh, T., Shanmugam, V., Guo, X., Lim, S., Filonik, O., Herzig, E., Buschbaum, P., Swamy, V., Chien, S., Mhaisalkar, S., & Mathews, N. (2018). Enhancing moisture tolerance in efficient hybrid 3D/2D perovskite photovoltaics. *Journal of Materials Chemistry A*, 6(5), 2122–2128.
- Lee, S. M., Jung, H., Park, W. I., Lee, Y., Koo, E., & Bang, J. (2018). Preparation of Water-Soluble CsPbBr<sub>3</sub> Perovskite Quantum Dot Nanocomposites via Encapsulation into Amphiphilic Copolymers. *Chemistry Select*, 3(40), 11320–11325. <https://doi.org/10.1002/slct.201802237>
- Papavassiliou, G. C. (1997). Three- and low-dimensional inorganic semiconductors. *Progress in Solid State Chemistry*, 25(3–4), 125–270. [https://doi.org/10.1016/S0079-6786\(97\)80886-2](https://doi.org/10.1016/S0079-6786(97)80886-2)
- Qin, C., Sandanayaka, A., Zhao, C., Matsushima, T., Zhang, D., Fujihara, T., & Adachi, C. (2020). Stable room-temperature continuous-wave lasing in quasi-2D perovskite films. *Nature*, 585, 53–57. <https://doi.org/10.1038/s41586-020-2621-1>
- Tan, Z., Wu, Y., Hong, H., Yin, J., Zhang, J., Lin, L., Wang, M., Sun, X., Sun, L., Huang, Y., Liu, K., Liu, Z., & Peng, H. (2016). Two-Dimensional (C<sub>4</sub>H<sub>9</sub>NH<sub>3</sub>)<sub>2</sub>PbBr<sub>4</sub> Perovskite Crystals for High-Performance Photodetector. *Journal of the American Chemical Society*, 138(51), 16612–16615. <https://doi.org/10.1021/jacs.6b11683>
- Wang, A., Guo, Y., Zhou, Z., Niu, X., Wang, Y., Muhammad, F., Li, H., Zhang, T., Wang, J., Nie, S., & Deng, Z. (2019). Aqueous acid-based synthesis of lead-free tin halide perovskites with near-unity photoluminescence quantum efficiency. *Chemical Science*, 10(17), 4573–4579. <https://doi.org/10.1039/c9sc00453j>
- Xing, G., Wu, B., Wu, X., Li, M., Du, B., Wei, Q., Guo, J., Yeow, E., Sum, T., & Huang, W. (2017). Transcending the slow bimolecular recombination in lead-halide perovskites for electroluminescence. *Nature Communications*, 8(14558). <https://doi.org/10.1038/ncomms14558>
- Yang, X., Ma, L.-F., & Yan, D. (2019). Facile synthesis of 1D organic–inorganic perovskite micro-belts with high water stability for sensing and photonic applications. *Chemical Science*, 10, 4567–4572. <https://doi.org/10.1039/C9SC00162J>